Experimental estimation of the location of liquid-liquid critical point for polyol aqueous solutions

Yoshiharu Suzuki[a)]
Research Center for Advanced Measurement and Characterization, National Institute for Materials Science (NIMS), Namiki 1-1, Tsukuba, Ibaraki 305-0044, Japan

(Received 2 August 2018; accepted 1 November 2018; published online 26 November 2018)

To solve a mystery of low-temperature liquid water, a liquid-liquid critical point (LLCP) hypothesis that the two kinds of waters, low-density and high-density liquids (LDL and HDL), and a critical point relating to the two waters exist is thought to be the most realistic idea. However, there is no conclusive evidence showing the existence of LLCP. I measured the polyamorphic volume changes of the glassy dilute polyol (ethylene glycol, glycerol, *meso*-erythritol, xylitol, and D-sorbitol) aqueous solutions during the compression and decompression processes and estimated the location of LLCP for the polyol aqueous solution by a new analysis of the concentration dependence of polyamorphic transition. The LLCP of glycerol aqueous solution around 150 K is estimated to be around 0.045 GPa and around 0.135 molar fraction. This indicates that the solvent water in the glycerol aqueous solution at 1 atm changes continuously from the LDL-like state to the HDL-like state with the increase of solute concentration. The concentration region in which the crossover between LDL-like solvent water and HDL-like solvent water occurs is located near the region that the liquid-liquid transition line is extended to the concentration axis at 1 atm. Moreover, the formation of LDL-like solvent water relates deeply to the homogeneous nucleation of ice Ih in the polyol aqueous solution. This conclusion shows that the LLCP hypothesis of water has an important implication for understanding the dynamics of aqueous solution such as solubility, hydration, segregation, aggregation of solute, nucleation of ice Ih, glass formation, glass transition, and so on. *Published by AIP Publishing.* https://doi.org/10.1063/1.5050832

I. INTRODUCTION

Water is a biogenic material and plays important roles for life activity of living things. Most biochemical activity in living things occurs under the liquid-water environment. However, the nature of liquid water is not fully understood. Water is not simple liquid and displays anomalous properties at low temperatures.[1] For instance, the density becomes maximum at 277 K (~4° C) and the heat capacity increases rapidly at low temperatures. The theory which explains the anomalous behavior of water successfully is not established yet.

Recent experimental, theoretical, and computer simulation studies relating to the supercooled liquid water and the discovery of two kinds of glassy waters (low-density and high-density amorphous ices: LDA and HDA) strongly suggest a liquid-liquid critical point (LLCP) hypothesis of water; two kinds of liquids (low-density and high-density liquid waters; LDL and HDL) exist, and a critical point relating to the two liquid waters (a liquid-liquid critical point: LLCP) is predicted.[1–3] Based on the LLCP hypothesis, the relation between the anomalous behaviors of liquid water and the fluctuation between LDL- and HDL-states which is generated around the LLCP are discussed actively, but cautiously, in the experimental,[4–10] theoretical,[11–13] and computer-simulation[14–19] fields.

For proving the LLCP hypothesis of water, it is necessary to measure the liquid-liquid critical phenomena of water directly. So far, many experimental scientists[4–10] have tried the direct observation of the critical phenomena near the LLCP, for example, the divergence of the heat capacity and the divergence of the compressibility at the LLCP. However, it is thought that the direct observation of LLCP will be difficult experimentally. This is because the LLCP will exist in the supercooled region in which the crystallization occurs easily and rapidly (the so-called "no-man's land"). Moreover, it may be impossible to determine the precise location of LLCP because of the metastability of supercooled water.[12,20] Actually, there is no conclusive evidence showing the existence of LLCP experimentally, as far as I know.

On the other hand, the many findings, which are derived from experimental studies for supercooled liquid water near the expected location of LLCP and two amorphous ices near their glass transition temperatures, support strongly the validity of LLCP hypothesis although they are the indirect pieces of experimental evidence.[4–7] The accurate measurement of the compressibility of supercooled liquid water under high pressures by Mishima[10] and the measurement of the melting curve of high-pressure ices in the no-man's land by Mishima *et al.*[4,5] have been performed. The experimental results have suggested strongly that the LLCP of pure water exists at ~0.05 GPa at ~223 K.[10] The LLCP location of water agrees with the LLCP

[a)]Author to whom correspondence should be addressed: suzuki.yoshiharu@nims.go.jp. Telephone: +81-29-860-4877.

location proposed by Holten *et al.*[11] In the present stage, the LLCP hypothesis of water may be plausible although there is no conclusive evidence.

The addition of solute to water and the confinement of water inside nanometer space tend to inhibit the crystallization of water. The experimental studies of the LLCP hypothesis of water using the aqueous solution system[21–25] and the confined water system[26–29] have been attempted. By using these systems, there is a possibility that the LLCP emerges out of the no-man's land. Actually, the distinct polyamorphic transition of dilute glycerol (GL) aqueous solution has been observed around 150 K which is higher than the glass transition temperature of pure LDA, ~136 K.[23] In this system, the polyamorphic transition between low- and high-density states under pressure is clearer than the LDA-HDA transition of pure water. In particular, it is able to observe the decompression curve of the low-density state in the wider low-pressure region. However, the direct observation of LLCP has not yet been reported.

The study of the polyamorphic behavior of solvent water in the aqueous solution has implications for the verification of the LLCP hypothesis of pure water as well as for the understandings of the static and dynamical interactions between the complex molecules, such as biomolecules and polymers, and the hydration water surrounding the molecules. There are several reports discussing the polyamorphic behavior of aqueous solutions from a viewpoint of LLCP hypothesis.[21–25,30–48] However, the relationship between the solute and the polyamorphic behavior of solvent water, for example, the effects of solute on the polyamorphic transition of solvent water and on the polyamorphic state of solvent water, is little understood.

Previously, we have examined the polyamorphic transition of glassy dilute ethylene glycol (EG), glycerol (GL), *meso*-erythritol (ER), xylitol (XY), and D-sorbitol (SO) aqueous solutions under pressure.[23,25] We have shown that there are two kinds of glassy forms, low-density glassy solution and high-density glassy solution, and then that two glassy solutions mutually transform with the change in pressure. It is verified using Raman spectroscopy that the hydrogen-bonded network structure of solvent water in the low-density glassy solution is similar to that of LDA and the hydrogen-bonded network structure of solvent water in the high-density glassy solution is similar to that of HDA. The transition between the low-density glassy solution and the high-density glassy solution relates to the LDA-HDA transition of pure water. The polyamorphic transition of GL aqueous solution has been supported by the computer simulation study of Jahn *et al.*[37] and the experimental study of Bachler *et al.*[38]

The existence of polyol solutes affects the polyamorphic behavior of solvent water.[23,25] As the solute concentration increases, the polyamorphic transition shifts toward the lower-temperature side. Moreover, with the increase of solute concentration, the slope of the stepwise volume change during the polyamorphic transition becomes gentler and the gap of the stepwise volume change that is the difference in the volume between the low-density state and the high-density state becomes smaller. When the solute concentration increases further and approaches a given value, the stepwise volume change relating to the polyamorphic transition disappears and the compression and decompression curves of volume become monotonous. This suggests that the LLCP of aqueous solution exists near the solute concentration at which the stepwise volume change disappears. Previously we have roughly estimated that the stepwise volume change of the GL aqueous solution at 150 K disappears at $x = \sim 0.12$, where the x stands for the solute molar fraction. We have inferred from the x dependence of the polyamorphic transition that the LLCP of the GL aqueous solution at 150 K is located at $x = 0.12$–0.15 at 0.03–0.05 GPa. However, the estimation of the location of LLCP is rough. The reason is that as the x increases, the stepwise volume change of the compression and decompression curves becomes extremely obscurer. Therefore, it is difficult to determine the correct x at which the stepwise volume change disappears.

In this study, I measured the compression and decompression curves of precise specific volume for the EG, GL, ER, XY, and SO aqueous solutions and estimated the location of the LLCP of polyol aqueous solutions experimentally using a new analysis method of the compression and decompression curves. Moreover, the polyamorphic state of solvent water in the glassy glycerol-D_2O solution at 1 atm was examined using Raman spectroscopy. I will discuss the relationship between the estimated location of LLCP and the polyamorphic state of solvent water in the GL aqueous solution at 1 atm. In this paper, I will mainly discuss the results obtained from the GL aqueous solution. The results obtained from other polyol aqueous solutions except for the GL aqueous solution are described in the supplementary material because the effect of concentration on the polyamorphic behavior has the same tendency in the polyol aqueous solutions.

II. SAMPLE AND EXPERIMENTAL METHOD

A. Polyol substance

The polyol solutes used in this study are ethylene glycol (EG), glycerol (GL), *meso*-erythritol (ER), xylitol (XY), and D-sorbitol (SO). EG, GL, and ER are purchased from Wako Pure Chemical Industries LTD. XY and SO are purchased from Sigma-Aldrich Co. The number of OH groups and the number of carbon atoms in a polyol molecule are increased by one in the order of EG_2, GL_3, ER_4, XY_5, and SO_6, where the subscript stands for the number of OH groups or the number of carbon atoms.

B. Preparation of the solution sample for the specific volume measurement

The polyol substance was mixed with high-purity H_2O (Millipore: Direct-Q UV). The solute concentration, x, of EG, GL, ER, XY, and SO aqueous solution is in the range of 0.03–0.18, 0.02–0.15, 0.02–0.05, 0.02–0.08, and 0.02–0.07, respectively. Here the x stands for a ratio of the solute molar number to the sum of the solute molar number and water molar number. In order to hinder the crystallization of dilute aqueous solution, the polyol aqueous solutions were emulsified. The emulsion sample was made by high-speed blending the 1 g of

sample solution and a matrix (0.75 g of methylcyclohexane, 0.75 g of methylcyclopentane, and 50 mg of sorbitan tristearate) for 1 min using a homogenizer (OMNI International: Omni TH) with 30 000 rpm. The emulsion size is 1-10 μm in diameter. In order to compare the present experimental results with the previous results of polyol aqueous solutions and pure water, the same emulsification procedure was used.[23,25] The influence of the emulsification procedure on the polyamorphic behavior of pure water and aqueous solution has been reported by Hauptmann *et al.*[49] According to their report, the emulsification procedure in this study has little influences on the freezing and transition of aqueous solution.

C. Pressure apparatus

A piston-cylinder high-pressure apparatus and an indium container were used for the high-pressure experiment and for the preparation of the high-density glassy sample. The cylinder temperature, T_{cy}, was measured by using an alumel-chromel thermocouple attached on the cylinder and was controlled by the balance of the attached heater and the atmosphere of cold nitrogen gas. The volume of the indium container with the emulsified sample was calculated from the change of the piston displacement with the change in pressure. The error of pressure, caused by the friction between piston and cylinder, was corrected by using the compression and decompression curves of the indium container without the sample that was obtained in the same experimental condition. The evaluation of the pressure correction has been described in Ref. 23.

D. Preparation of a high-density glassy sample for the measurement of specific volume

In order to prepare a homogeneous high-density glassy sample consisting of the HDA-like solvent water as the starting sample, the dilute aqueous solution was compressed at 0.3 GPa at room temperature and then the sample was rapidly cooled down to 77 K [Fig. 1(a)]. In general, when cooling the dilute aqueous solution at 1 atm, a part of solvent water crystallizes to ice Ih and then the segregation to the water-rich crystalline part and the solute-rich glassy part occurs. Therefore, the existence of concentration inhomogeneity complicates the analysis of polyamorphic transition. In order to examine the polyamorphic behavior of dilute aqueous solution, it is necessary to prepare the glassy sample in which the solute molecules disperse homogeneously. Previously, we have vitrified the emulsified pure water[50] and the bulky dilute aqueous solution, such as LiCl aqueous solution[22,51] and GL aqueous solution,[23–25] by a rapid cooling under pressure and then examined the state of the glassy water and glassy solvent water. The glassy state of water relates closely to the state of high-density amorphous ice.[50–52]

About 1.5 ml of the fresh emulsified sample was sealed in the indium container at 1 atm, compressed to 0.3 GPa at room temperature by using the piston-cylinder apparatus, and then cooled to 77 K at a cooling rate of ~40 K/min [Fig. 1(a)]. In this study, the EG and GL aqueous solutions below $x = 0.02$ and the ER, XY, and SO aqueous solutions below $x = 0.01$ crystallize. Therefore, I examined the polyamorphic behavior of the EG and GL aqueous solutions above $x = 0.03$ and of the ER, XY, and SO aqueous solutions above $x = 0.02$. Previously, we have measured the change in the sample temperature during the cooling process and verified that there is no exothermic event caused by the crystallization of solvent water. I have checked also using Raman spectroscopy that the sample made by the high-pressure cooling process without the exothermic event contains no crystalline parts.[23] Moreover, in the previous study for the high-density glassy glycerol aqueous solution made by the same preparation condition,[23,25] it is found that the glycerol solutes disperse homogeneously because of the good reproducibility of repetitive polyamorphic transition; suggesting strongly that the high-density glassy sample is a homogeneous glass. The check of the crystallization of the sample using the X-ray diffraction method is desirable, but not done in this study.

E. Measurement of the specific volume

A typical experimental protocol for the measurement of specific volume in this study is shown in Fig. 1(a). The

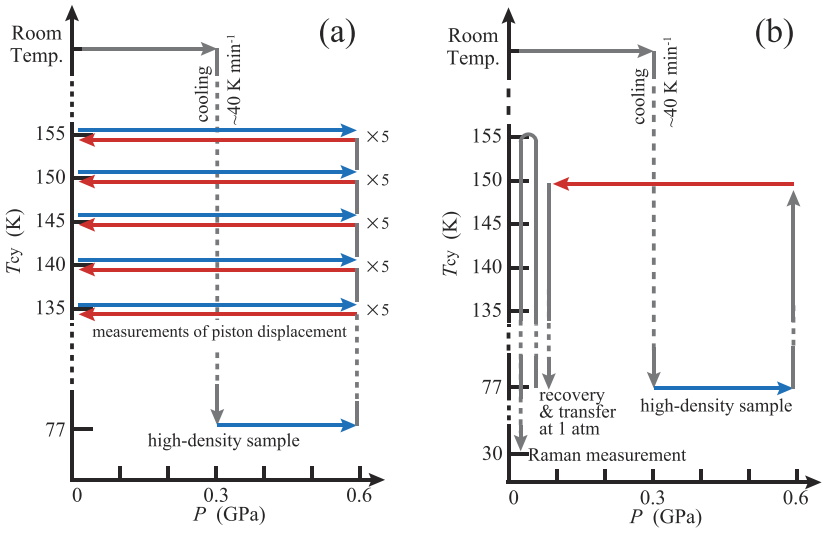

FIG. 1. Temperature-pressure steps for the preparation of the high-density glassy sample and for the experimental process. (a) The temperature-pressure steps for the measurement of polyamorphic transition. (b) The temperature-pressure steps for the Raman measurement.

high-density glassy sample made by cooling at 0.3 GPa was further compressed to 0.6 GPa at 77 K, and the piston-cylinder with the sample was heated to a given T_{cy}. The sample at the T_{cy} was decompressed from 0.6 to 0.01 GPa, kept at 0.01 GPa for about 2 min and then compressed to 0.6 GPa. During the decompression and compression processes, the change in the piston displacement, d, was measured. This measurement was repeated five times at the same T_{cy}. The T_{cy} was changed in the order of 135, 140, 145, 150, and 155 K as shown in Fig. 1(a). The decompression rate and compression rate may affect the experimental results of the polyamorphic behavior such as the transition pressure. Therefore, the decompression rate and compression rate in this experiment were fixed at ~1.6 MPa/s which was the same as the rate used in the previous studies. The effect of the change of sample temperature caused by the polyamorphic transition on the T_{cy} is little because the amount of sample is remarkably less than that of the piston-cylinder.

The specific volume of aqueous solution was calculated by subtracting the volume of the indium container and the volume of the emulsion matrix from the measured volume in consideration of the pressure and temperature effects. The compression and decompression curves of the indium container at 135, 140, 145, 150, and 155 K were measured in advance. In addition, the pressure dependences of the specific volume of the emulsion matrix at 135, 140, 145, 150, and 155 K in the compression and decompression processes were measured in advance. The specific volume of the sample was calculated using this information considering the pressure and temperature effects. We have verified that there is no transition of the indium container between 0.001 and 0.6 GPa and there is no transition of the emulsion matrix.[23] The error of the absolute value of specific volume is estimated to be ±~2%.

The five times average of the compression curve, V_c, and the five times average of the decompression curve, V_d, of specific volume for the EG, GL, ER, XY, and SO aqueous solutions are shown in Fig. 2(a) and Figs. S1(a)–S1(e). The glassy sample at the higher T_{cy} crystallizes during or after the polyamorphic transition from the high-density to low-density state in the decompression process. The crystalline sample can be checked by the compression curve which does not have the stepwise volume change relating to the polyamorphic transition. The crystalline sample was not used. For example, the glassy EG aqueous solution crystallizes after the polyamorphic transition in the decompression process at T_{cy} = 150 K. Therefore, the measurements for the EG aqueous solution were performed at T_{cy} = 145 K.

F. Sample preparation for the Raman spectroscopic study

The GL was mixed with D_2O (Wako Pure Chemical Industries LTD.). The non-emulsified GL aqueous solution was used. The x of GL aqueous solution ranges between 0.07 and 0.24. The bulky GL aqueous solution below x = 0.06 crystalized during the high-pressure cooling.

The thermal and pressure protocols of the glassy sample preparation for the Raman study are shown in Fig. 1(b). In order to prepare the high-density glassy GL aqueous solution first, the GL aqueous solution was compressed at 0.3 GPa at room temperature and then the sample was rapidly cooled down to 77 K. For making the low-density glassy sample at 150 K, the prepared high-density glassy sample was compressed up to 0.6 GPa, heated at 150 K, and then decompressed to 1 atm. The sample of low x was transformed into the low-density state during this decompression process. The glassy sample was cooled down to 77 K at 1 atm. The glassy sample with the indium container was recovered from the piston cylinder at 77 K, and the cap of the container was removed to expose the surface of the glassy sample. The recovered glassy sample

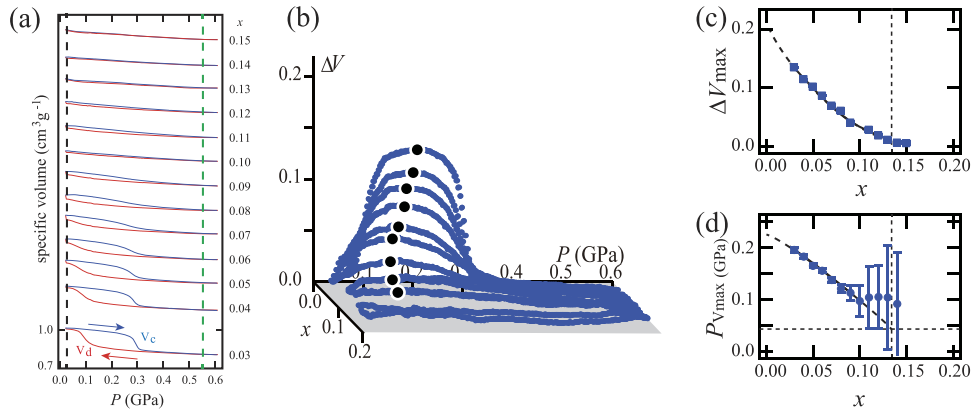

FIG. 2. The x dependence of polyamorphic transition for the GL aqueous solution at 150 K. (a) The compression and decompression curves (V_c and V_d) of specific volume for the GL aqueous solutions of x = 0.03-0.15 at 150 K were measured in the pressure range between 0.01 and 0.60 GPa. The V_c and V_d are presented by red and blue lines, respectively. The V_c and V_d except for ones of x = 0.03 are shifted vertically for clarity. The vertical broken lines indicate the location of 0.01 and 0.55 GPa. (b) The x dependence of ΔV for the GL aqueous solution at 150 K is shown. Black closed circles represent the maximum of ΔV, ΔV_{max}. As the x increases, the dome part of ΔV is squashed and the ΔV_{max} becomes small. When the x reaches around 0.13, the dome part of ΔV disappears and the ΔV becomes almost flat. (c) The ΔV_{max} is plotted as a function of x. The solid curve is the fitted curve and the broken curve is the extrapolated curve. The position of vertical broken line stands for the x_{LLCP} (=0.135). The error of ΔV_{max} is small, and the error bar is hidden behind the square mark. (d) The P_{Vmax} is plotted as a function of x. The solid curve is the fitted curve, and the broken curve is the extrapolated curve. The position of the vertical broken line stands for the x_{LLCP} (=0.135). The position of the horizontal broken line stands for the P_{LLCP} (=0.045 GPa). The crossing point of the vertical and horizontal broken lines may be the location of LLCP for the GL aqueous solution at 150 K.

was placed on a cryostat with a temperature controller for the Raman spectroscopic measurement. After the glassy sample was annealed at 155 K at 1 atm for the structural relaxation, the sample was cooled to ~30 K quickly and then the Raman measurement was performed at ~30 K.

G. Raman spectroscopic study

The Raman spectroscopic measurement was performed using a microscopic Raman spectrometer system (Jobin Yvon Inc. T-64000). The exciting light source was an argon ion gas laser operating at 488 nm with a power of 400 mW. The laser light via the optical system was attenuated, and the laser power in front of the sample was about 20 mW. Therefore, we can ignore the elevation of sample temperature caused by the laser irradiation.

The intensity of the Raman scattered radiation polarized parallel to the incident light, $I(\nu)$, was recorded in the frequency region from 2000 to 3000 cm^{-1} with the resolution of 0.2 cm^{-1}, where ν is the Raman frequency.

The polyamorphic state of solvent water was identified by the Raman profile of OD-stretching modes in the range of 2200–2700 cm^{-1}. Assuming the tentative mode assignment of pure glycerol,[53] the vibration modes relating to the side groups in a glycerol molecule, for example, the OH- and CH_2-stretching modes, appear in 2700-3700 cm^{-1}. Therefore, the effect of vibrational modes in the glycerol molecule on the OD-stretching vibrational modes is little.

III. ANALYSIS AND RESULTS

Figure 2(a) shows the compression curve, V_c, and decompression curve, V_d, of specific volume for the GL aqueous solution of x = 0.03-0.15 at 150 K. The V_c and V_d for the other polyol aqueous solutions are shown in Fig. S1. For the GL aqueous solution of x = 0.03, the polyamorphic stepwise volume changes clearly appear around 0.28-0.30 GPa in the compression process and around 0.07-0.10 GPa in the decompression process. As the x increases, the slope of the stepwise volume change becomes smaller and the difference in specific volume between the low-density sample and the high-density sample becomes smaller. Above x = 0.12, the stepwise volume change seems to disappear. The effect of the addition of solute on the polyamorphic transition was similar among the EG, GL, ER, XY, and SO aqueous solutions (Fig. S1). However, the x at which the polyamorphic transition disappears becomes smaller in the order of EG, GL, ER, XY, and SO aqueous solution. The solute nature dependence of the polyamorphic transition agrees with the previous result.[25]

In order to discuss the polyamorphic transition of GL aqueous solution more quantitatively, I introduce a new parameter, $\Delta V = (V_c - V_d)/V_{c=0.01GPa}$, where $V_{c=0.01GPa}$ stands for the V_c at 0.01 GPa (see the supplementary material and Fig. S2). Figure 2(b) shows the ΔV for the GL aqueous solutions of x = 0.03-015 at 150 K. The ΔV for the GL aqueous solution in the low x region has a dome-type part indicating that the polyamorphic transition occurs. The shape of the dome part characterizes the behavior of polyamorphic transition. For example, the maximum value of the dome part of ΔV, ΔV_{max}, corresponds to the gap of stepwise polyamorphic transition and indicates a volume ratio of the low-density sample and the high-density sample. Indeed, the ΔV_{max} calculated from the LDA-HDA transition of pure water at ~135 K is about 0.2 (see the supplementary material and Fig. S8). This value agrees with the volume ratio of LDA and HDA reported by Mishima *et al.*[54,55]

In addition, the pressure of ΔV_{max}, P_{Vmax}, relates to the location of the equilibrium coexistent line of low-density and high-density states. The dome part of ΔV is quite asymmetric, and the P_{Vmax} is different from the pressure previously defined by the middle point between the pressure of polyamorphic transition from the low-density to high-density state and the pressure of polyamorphic transition from the high-density to low-density state.[23,25] Therefore, the P_{vmax} may not be the correct pressure of equilibrium liquid-liquid transition (LLT).

The full width half maximum of the dome part of ΔV corresponds to the hysteresis size of polyamorphic transition, and the slope of the inclined part of the dome corresponds to the slope of stepwise volume change during the polyamorphic transition (see the supplementary material).

The black points in Fig. 2(b) represent the ΔV_{max} for the GL aqueous solution of x = 0.03-015 at 150 K. As the x increases, the dome part of ΔV is squashed and the ΔV_{max} becomes small. When the x reaches around 0.13, the dome part of ΔV disappears and the shape of ΔV becomes almost flat. The x dependences of ΔV for EG, ER, XY, and SO aqueous solutions show a similar tendency (Fig. S3).

For discussing more qualitatively, the ΔV_{max} for the GL aqueous solution is plotted as a function of x in Fig. 2(c). As the x increases, the ΔV_{max} decreases and then the change of ΔV_{max} is leveled in the higher concentration region above x = 0.135. This indicates that the polyamorphic transition of the GL aqueous solution at 150 K disappears around x = 0.135. Therefore, I determine that the concentration at which the change of ΔV_{max} begins to become flat is the x of LLCP, x_{LLCP}.

Using the same analysis of the ΔV_{max}–x curve, I estimated the x_{LLCP} for the EG, ER, XY, and SO aqueous solutions (Fig. S4). The values of x_{LLCP} for EG, ER, XY, and SO aqueous solutions are 0.145, 0.08, 0.065, and 0.055, respectively. The magnitude correlation of x_{LLCP} is consistent with the previous estimation.[25]

On the other hand, the value of ΔV_{max} extrapolated to x = 0 becomes ~0.2 as presented in Fig. 2(c). The extrapolated ΔV_{max} for the other polyol aqueous solutions is also ~0.2 (Fig. S4). These values agree well with the ΔV_{max} calculated from the LDA-HDA transition of pure water at ~135 K, ~0.2 (Fig. S8).

Next, the P_{Vmax} for the GL aqueous solution at 150 K is plotted as a function of x in Fig. 2(d). The P_{Vmax} decreases monotonously with the increase of x. The analytical errors of P_{Vmax} in the concentration region above x = 0.11 become large. This is because the shape of the ΔV of GL aqueous solution above x = 0.11 is almost flat as shown in Fig. 2(b), and the determination of the correct ΔV_{max} in the dome part is difficult. Therefore, I carried out the fitting analysis using the P_{Vmax} below x = 0.10. The fitted broken curve in Fig. 2(d)

TABLE I. Location of LLCP for polyol aqueous solutions.[a]

Solute	T (K)	x_{LLCP}	P_{LLCP} (GPa)	x_{TH}
EG	145	0.145	0.055	0.17
GL	150	0.135	0.045	0.13
ER	150	0.08	0.05	...
XY	150	0.065	0.055	0.11
SO	150	0.055	0.050	0.10

[a]The data in Table I correspond to just one point along a location of LLCP as shown in the green dashed line of Fig. 3.

shows that the value of P_{Vmax} at $x_{LLCP} = 0.135$ is ~0.045 GPa. Therefore, I decide that the pressure of LLCP, P_{LLCP}, for the GL aqueous solution at 150 K is ~0.045 GPa. As a result, the LLCP location of the GL aqueous solution of 150 K is $x_{LLCP} = 0.135$ and $P_{LLCP} = 0.045$ GPa. This does not deviate from the previous rough estimation of the LLCP location of GL solution at ~150 K ($x_{LLCP} = 0.12$–0.15 and $P_{LLCP} = 0.03$–0.05 GPa).[23]

Using the same analysis method, I estimated that the P_{LLCP} for the EG, ER, XY, and SO aqueous solutions is 0.055, 0.050, 0.055, and 0.050 GPa, respectively (Fig. S5). The LLCP locations for polyol aqueous solutions are summarized in Table I.

The x_{LLCP} for the polyol aqueous solutions reduces in the order of EG, GL, ER, XY, and SO aqueous solution and becomes smaller with the increase of the number of OH groups in a polyol solute molecule. The x_{LLCP} seems to relate to the number of OH groups in a polyol solute. Indeed, I have demonstrated that when the x is replaced by the concentration of the OH group relating to the polyol solute, the solute nature dependence of the polyamorphic behavior, for example, the slope of LLT line and the location of LLCP, becomes small.[25] This suggests that the hydrogen bonded interaction between solute and solvent water affects the polyamorphic behavior of the solvent water in the aqueous solution. The existence of the OH group may reduce the stability of the LDA-like hydrogen bonded network structure of solvent water. However, it is difficult to clarify the relation between the polyamorphic state of solvent water and the hydrogen bonded interaction between the solute and water from the present experiment.

The value at which P_{Vmax} of the GL aqueous solution in Fig. 2(d) is extrapolated to $x = 0$ seems to be ~0.225 GPa. Similarly, the extrapolated values of P_{Vmax} to $x = 0$ for the EG, ER, XY, and SO aqueous solutions are ~0.24, ~0.23, ~0.23, and ~0.23 GPa, respectively (Fig. S5). These values of P_{Vmax} extrapolated to $x = 0$ are almost the same within the error (±~0.01), and the average value is 0.23 GPa. Assuming that the P_{Vmax} at $x = 0$ corresponds to the pressure of the equilibrium boundary of LDA and HDA, although the P_{Vmax} is not the correct pressure of LLT, the average value agrees with the previous result (~0.23 GPa)[23,25] that is slightly larger than the value (~0.20 GPa) estimated by Mishima *et al.*[2]

IV. DISCUSSION

The schematic P-T-x diagram of the polyamorphic state of solvent water in the GL aqueous solution is drawn in Fig. 3. It is found that the P_{LLCP} of the GL aqueous solution at 150 K is ~0.045 GPa and the LLCP exists in the positive pressure region. According to the reports by Mishima[10] and Holten *et al.*,[11] the P_{LLCP} of H_2O is 0.03-0.05 GPa. The P_{LLCP} of pure water and the P_{LLCP} of the GL aqueous solution at 150 K are same within experimental error. This indicates that the effect of the addition of GL solute is the shift of the LLT toward the lower temperature side. In short, the location of LLCP seems to shift toward the lower temperature side with the increase of x as shown by a green broken curve in Fig. 3.

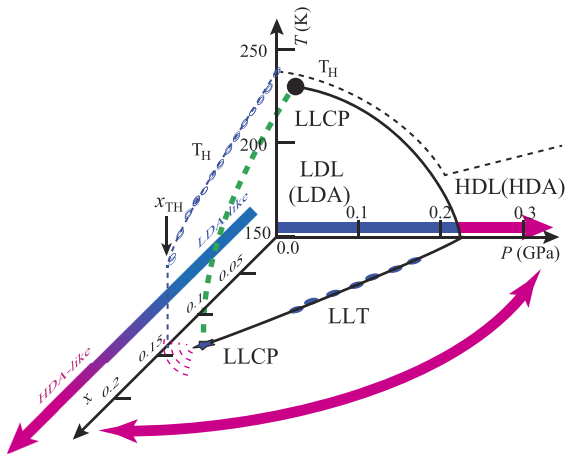

FIG. 3. The schematic P-T-x diagram of the solvent water in the GL aqueous solution. The polyamorphic P-T diagram of pure water at $x = 0$ has been proposed by Mishima and Stanley.[2] The T_H of GL aqueous solution at 1 atm[25] is plotted in the T-x plane at 1 atm. The T_H curve becomes perpendicular to the x axis at x_{TH}. The LLCP and the LLT lines which are estimated in this study are drawn in the P-x plane at 150 K. The LLCP may shift toward the lower temperature side with the increase of x as shown by a green broken curve. The region along the extension of LLT line is drawn as the red broken arcs in the P-x plane. The color of arrows in the T-x plane at 1 atm and the P-T plane at $x = 0$ represents the change in the polyamorphic state of solvent water, where the blue and red stand for the LDA-like solvent water and the HDA-like solvent water, respectively. The red arc arrow in the P-x plane indicates that the state of solvent water in the highly concentrated GL aqueous solution at 1 atm is equivalent to the state of HDA.

In addition, Fig. 3 suggests that the state of solvent water in the lower pressure region of the LLT line on the P-x plane is LDA-like and the state of solvent water in the higher pressure region of the LLT line is HDA-like. Therefore, the GL aqueous solution at 1 atm above $x = 0.15$ is located in the higher pressure region of the LLT line, and the solvent water is categorized into the HDA-like group. This suggests that the solvent water in the GL aqueous solution at 1 atm changes from LDA-like to HDA-like continuously with the increase of x as shown by an arrow on the T-x plane in Fig. 3. On the other hand, in the case of pure water the LDA is transformed discontinuously into HDA at the LLT line with the increase of pressure as shown by an arrow on the P-T plane in Fig. 3. This suggests that the effect of the addition of GL solute on the polyamorphic state of water is equivalent to the effect of the application of pressure. This is similar to the result for the electrolyte aqueous solution at room temperature by Leberman and Soper.[56]

Here, the state of the solvent water at 1 atm in the region of $x = 0.13$-0.15 may correspond to a LDL-HDL supercritical state near the LLCP. In order to verify the LDA-HDA crossover of solvent water at 1 atm with the change in x, I examined the

x dependence of the specific volume of glassy GL aqueous solution at 150 K at 0.01 GPa and the x dependence of the OD-stretching Raman mode of solvent water in the glassy GL-D_2O sample at 155 K at 1 atm.

The specific volume of GL aqueous solution at 0.01 GPa at 150 K which is marked by the vertical black dashed line in Fig. 2(a) is plotted as a function of x in Fig. 4 (green closed circle). The numerical information of specific volume is shown in Table S1. If the solvent water is LDA and if this does not change regardless of the change of x, the specific volume will act as a blue curve in Fig. 4. The specific volume of pure LDA at 135 K at 0.01 GPa is 1.07 cm^3 g^{-1} in Fig. S8(a) and the specific volume of pure glycerol is assumed to be 0.7830 cm^3 g^{-1} that is the value of the specific volume of pure glycerol at room temperature at 1 atm. On the other hand, if the solvent water is HDA and if this does not change regardless of the change of x, the specific volume will behave as a red curve in Fig. 4. Here, the specific volume of pure HDA at 0.01 GPa is assumed to be 0.88 cm^3 g^{-1} that is estimated by the extrapolation of the V_d of pure HDA to 0.01 GPa in Fig. S8(a). Here, I assume that the solute does not affect the specific volume of aqueous solution with LDA-like (HDA-like) solvent water. However, the real specific volume of aqueous solution at high solute concentration deviates from the ideal specific volume such as the blue (red) line in Fig. 4 because of the complex interaction between solvent water and solute. I think that it is meaningful to consider the tendency of the change in specific volume from a viewpoint of the polyamorphic state of solvent water although the estimated red and blue lines are not real.

The measured specific volume of GL aqueous solution at 0.01 GPa (green closed circles) decreases continuously in the region between the blue and red curves with the increase of x. This indicates that the state of solvent water in the GL aqueous solution at 0.01 GPa at 150 K changes from the LDA-like state to the HDA-like state continuously with the increase of x. Moreover, this result suggests that the cause of the reduction of ΔV_{max} with the increase of x is the polyamorphic change of solvent water.

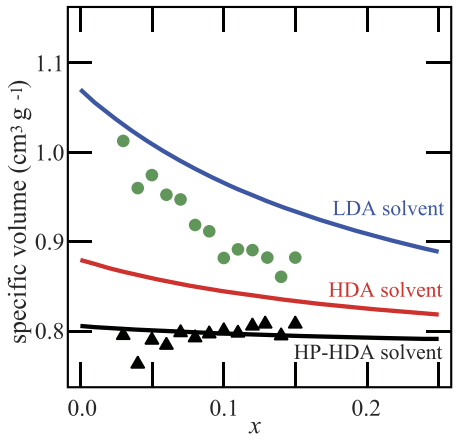

FIG. 4. The x dependences of the specific volume of GL aqueous solution at 150 K at 0.01 and 0.55 GPa. The closed circle and closed triangle stand for the specific volume at 0.01 and 0.55 GPa, respectively. Assuming that the solute does not influence on the state of solvent water, the specific volume of GL aqueous solution at 0.01 GPa with the solvent water of LDA changes like the blue solid curve. Similarly, the red solid curve is the change of the specific volume of GL aqueous solution at 0.01 GPa with the solvent water of HDA. The black solid curve is the change of the specific volume of GL aqueous solution at 0.55 GPa with the solvent water of HDA at 0.55 GPa.

The specific volume of GL aqueous solution at 0.55 GPa at 150 K which is marked by the green vertical dashed line in Fig. 2(a) is shown by the black triangle in Fig. 4. If the solvent water of HDA does not change regardless of the change of x, the specific volume will behave as shown by a black curve, where the specific volume of pure HDA at 0.55 GPa is 0.81 cm^3 g^{-1} [Fig. S8(a)]. The x dependence of the measured specific volume (black triangle) behaves like the black line, indicating that the state of solvent water in the GL aqueous solution at high pressures is HDA-like regardless of the change of x. Considering that the V_c and V_d for the GL aqueous solution above $x_{LLCP} = 0.135$ shows the continuous change without the polyamorphic transition [Fig. 2(a)], the solvent water in the GL aqueous solution above $x_{LLCP} = 0.135$ at 1 atm connects continuously to the HDA of pure water at high pressures as shown by a red arc arrow in Fig. 3. In short, the solvent water in the highly concentrated GL aqueous solution is categorized into the HDA group.

The results derived from the x dependence of the specific volume for ER, XY, and SO aqueous solutions at 0.01 and 0.55 GPa show a similar tendency of the result for the GL aqueous solution (see Fig. S9).

Next, I examined the x dependence of the OD-stretching Raman spectra of glassy glycerol-D_2O solution at 1 atm; it corresponds to the Raman spectra of glassy solution near the vertical broken line of 0.01 GPa in Fig. 2(a). In order to avoid the overlap of OH stretching mode between H_2O and GL molecule, D_2O instead of H_2O was used as solvent water. There is a little isotope effect on the polyamorphic behavior of water.[5,24] The effect may be caused by the different properties between light water and heavy water.[57] However, the polyamorphic behavior between light water and heavy water is similar. Moreover, we have checked in the previous study that there is no effect of the hydrogen/deuterium exchange between glycerol and D_2O on the polyamorphic behavior.[24]

The x dependence of the OD-stretching Raman spectrum in 2200-2700 cm^{-1} is shown in Fig. 5. The glassy sample was annealed at 155 K at 1 atm for relaxing the high-pressure structure, and then the measurement of Raman spectrum was performed at ~30 K for clarifying the slight difference of the Raman profile between the LDA-like state and HDA-like state. The OD-stretching Raman profile for the GL aqueous solution of $x = 0.07$ is similar to that of pure LDA (D_2O) although the Raman profile is slightly distorted and although the position of the largest peak at ~2302 cm^{-1} shifts to the higher side than that of LDA (~2293 cm^{-1}). As the x increases, the position of largest peak shifts to the higher frequency side and the peak intensity becomes smaller. At $x = 0.24$, the OD-stretching Raman profile is almost similar to that of pure HDA (D_2O) which has the peak position at ~2338 cm^{-1}.[23] The change of Raman profile suggests that the state of solvent water in the GL aqueous solution at 1 atm changes continuously from the LDA-like state to the HDA-like state with the increase of x. This consists of the conclusion derived from the x dependence of specific volume as shown above.

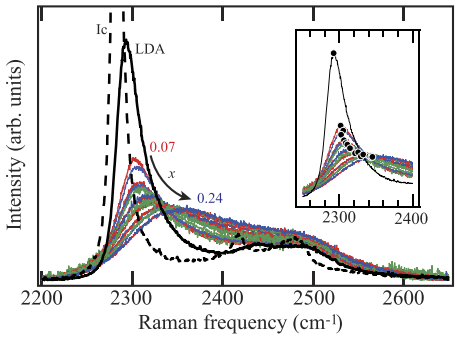

FIG. 5. The x dependence of the OD-stretching Raman spectra of solvent water in the GL-D_2O solution at 1 atm. The Raman spectra of LDA (D_2O) and crystalline ice Ic (D_2O) are presented by a black solid line and a black broken line, respectively. The black closed circle in an inset stands for the peak position of the largest OD-stretching vibrational mode.

The position of the largest peak around 2300-2350 cm^{-1} is plotted as a function of x in Fig. 6. The x dependence of the peak position shows a sigmoid curve, and the peak position increases sharply in the region of x = 0.13-0.19. This indicates that the polyamorphic state of solvent water in the GL aqueous solution at 1 atm changes from the LDA-like state to the HDA-like state drastically in the region of x = 0.13-0.19.

The peak position for the GL aqueous solution above x = 0.20 is larger than that for pure HDA. Previously, we have shown experimentally that the OH-stretching Raman spectrum of HDA which is relaxed under high pressures shifts toward the higher frequency side than that of HDA which is relaxed at 1 atm.[58] In addition, Leberman and Soper have suggested the equivalency between the salt effect on liquid water and the pressure effect on liquid water.[56] According to these experimental findings, the overshooting of the peak position suggests that the HDA-like solvent water in the GL aqueous solution at high molar fractions is similar to HDA under high pressures.

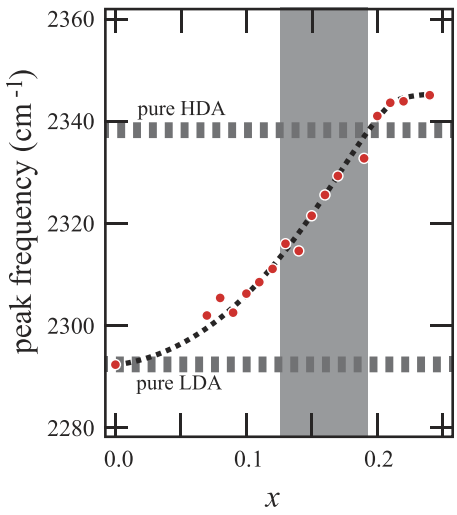

FIG. 6. The x dependence of the peak frequency of the largest OD-stretching vibrational mode for the GL-D_2O solution at 1 atm at 155 K. The broken curve is drawn for guide of eyes. The slope of the broken curve becomes largest in a gray region between x = 0.13 and 0.19. The horizontal broken lines stand for the peak frequencies of the largest OD-stretching vibrational mode of the pure LDA (~2293 cm^{-1}) and the pure HDA (~2338 cm^{-1}).

The x region in which the LDA-HDA crossover occurs in Fig. 6 seems to coincide with the x region that the LLT line in Fig. 3 is extended to the ambient pressure, x = 0.13-0.15. It is thought that the fluctuation between the two polyamorphic states of solvent water may become large in the region along an extension of LLT line from the LLCP to 1 atm.[26,59] This suggests that the LDA-HDA crossover of solvent water at 1 atm correlates closely with the polyamorphic fluctuation of the solvent water generated at the LLCP.

A homogeneous nucleation temperature, T_H, of GL aqueous solution at 1 atm[25] is drawn in the T-x plane of Fig. 3. The T_H decreases with the increase of x, and then the T_H curve becomes almost perpendicular at the x_{TH} = ~0.13 (Table I). This indicates that the GL aqueous solution below x_{TH} segregates into the crystalline ice Ih part and the concentrated glassy solution part at low temperatures and the GL aqueous solution above x_{TH} vitrifies homogeneously at low temperatures. As shown in Fig. 3, the x_{TH} is located near the region at which the LDA-HDA crossover of solvent water occurs. Similarly, the T_H for pure water at 1 atm is ~235 K and the location of T_H seems to exist near the region that the assumed LLT line of pure water is extended to 1 atm. Figure 3 shows that the region in which the homogeneous nucleation of ice Ih occurs agrees with the region in which the LDA-like (LDL-like) water is able to exist. The region of LDA-like water for the ER, XY, and SO aqueous solutions seems to agree with their homogeneous nucleation region (Fig. S10). This indicates that the nucleation of ice Ih which is a kinetic phenomenon relates closely to the formation of the LDL-like hydrogen-bonded network which is a thermodynamic phenomenon. The formation of the LDL-like hydrogen bonded network may be a necessary condition for the nucleation of ice Ih. This experimental finding strongly supports the suggestions that LDL is the precursor of nucleus of ice Ih.[30,60–62]

The P-T-x diagram of the polyamorphic state of solvent water in the GL aqueous solution in Fig. 3 is contradictory to the past report[63] that the LLT of solvent water has occurred in the GL-water solution of x = 0.178 at ~171 K at 1 atm. I think that the transition reported in Ref. 63 may be the crystallization relating to the fluctuation of solvent water near the LLCP.[23,39,64]

In conclusion, I examined the polyamorphic transition for the polyol aqueous solutions experimentally and estimated the location of LLCP as shown in Table I. The LLCPs are located in the positive pressure regions. The solvent water in the polyol aqueous solution at 1 atm changes from LDL-like to HDL-like continuously with the increase of x. The region at which the crossover between the LDL-like state and HDL-like state occurs agrees with the region in which the LLT line is extended to 1 atm. The crossover between the LDL-like solvent water and the HDL-like solvent water seems to be caused by the polyamorphic fluctuation of solvent water generated near the LLCP. This suggests a possibility that the local fluctuation of solute concentration, for example, the inhomogeneity of concentration induced by the phase separation of the binary mixture and by the self-aggregation of macromolecule, induces the changes of the polyamorphic state of solvent water. Conversely the polyamorphic change of solvent water induced by the temperature change may affect the

structure of solute.[24,44,45] Therefore, the polyamorphic fluctuation of solvent water in the aqueous solution may affect not only the behavior of aqueous solution but also the structure of solute such as polymer, biomolecule, and so on.

Considering the solvent water in the aqueous solution from a viewpoint of LLCP hypothesis of water, the state of solvent water can be classified into the LDL-like state and the HDL-like state. In short, the two types of water structures can exist around the solute. Therefore, the interaction between the LDL-like water and the solute should be different from the interaction between the HDL-like water and the solute, for example, the difference between the solubility of solute to LDL and the solubility of the solute to HDL. This indicates that the water polyamorphism relates closely to the dynamics of aqueous solution such as solubility, hydration, segregation, aggregation of solute, nucleation of ice Ih, glass forming, glass transition, and so on. I expect to understand the further relation between the aqueous solution and the water polyamorphism in the future water study.

SUPPLEMENTARY MATERIAL

The information of the new analysis method of polyamorphic transition and the experimental results for the polyol aqueous solutions except for the GL aqueous solution is shown in the supplementary material.

ACKNOWLEDGMENTS

I am grateful to Osamu Mishima and Izumi Nishio for precious discussion and careful review.

[1] P. G. Debenedetti, J. Phys.: Condens. Matter **15**, R1669 (2003).
[2] O. Mishima and H. E. Stanley, Nature **396**, 329 (1998).
[3] P. Gallo, K. Amann-Winkel, C. A. Angell, M. A. Anisimov, F. Caupin, C. Chakravarty, E. Lascaris, T. Loerting, A. Z. Panagiotopoulos, J. Russo, J. A. Sellberg, H. E. Stanley, H. Tanaka, C. Vega, L. Xu, and L. G. M. Pettersson, Chem. Rev. **116**, 7463 (2016).
[4] O. Mishima and H. E. Stanley, Nature **392**, 164 (1998).
[5] O. Mishima, Phys. Rev. Lett. **85**, 334 (2000).
[6] K. Amann-Winkel, C. Gainaru, P. H. Handle, M. Seidl, H. Nelson, R. Bohmer, and T. Loerting, Proc. Natl. Acad. Sci. U. S. A. **110**, 17720 (2013).
[7] J. A. Sellberg, C. Huang, T. A. McQueen, N. D. Loh, H. Laksmono, D. Schlesinger, R. G. Sierra, D. Nordlund, C. Y. Hampton, D. Starodub, D. P. DePonte, M. Beye, C. Chen, A. V Martin, A. Barty, K. T. Wikfeldt, T. M. Weiss, C. Caronna, J. Feldkamp, L. B. Skinner, M. M. Seibert, M. Messerschmidt, G. J. Williams, S. Boutet, L. G. M. Pettersson, M. J. Bogan, and A. Nilsson, Nature **510**, 381 (2014).
[8] K. H. Kim, A. Späh, H. Pathak, F. Perakis, D. Mariedahl, K. Amann-Winkel, J. A. Sellberg, J. H. Lee, S. Kim, J. Park, K. H. Nam, T. Katayama, and A. Nilsson, Science **358**, 1589 (2017).
[9] F. Perakis, K. Amann-Winkel, F. Lehmkühler, M. Sprung, D. Mariedahl, J. A. Sellberg, H. Pathak, A. Späh, F. Cavalca, D. Schlesinger, A. Ricci, A. Jain, B. Massani, F. Aubree, C. J. Benmore, T. Loerting, G. Grübel, L. G. M. Pettersson, and A. Nilsson, Proc. Natl. Acad. Sci. U. S. A. **114**, 8193 (2017).
[10] O. Mishima, J. Chem. Phys. **133**, 144503 (2010).
[11] V. Holten, C. E. Bertrand, M. A. Anisimov, and J. V. Sengers, J. Chem. Phys. **136**, 094507 (2012).
[12] V. Holten and M. A. Anisimov, Sci. Rep. **2**, 713 (2012).
[13] V. Holten, J. Kalová, M. A. Anisimov, and J. V. Sengers, Int. J. Thermophys. **33**, 758 (2012).
[14] P. H. Poole, F. Sciortino, U. Essmann, and H. E. Stanley, Nature **360**, 324 (1992).
[15] J. C. Palmer, F. Martelli, Y. Liu, R. Car, A. Z. Panagiotopoulos, and P. G. Debenedetti, Nature **510**, 385 (2014).
[16] R. S. Singh, J. W. Biddle, P. G. Debenedetti, and M. A. Anisimov, J. Chem. Phys. **144**, 144504 (2016).
[17] J. L. F. Abascal and C. Vega, J. Chem. Phys. **133**, 234502 (2010).
[18] T. Sumi and H. Sekino, RSC Adv. **3**, 12743 (2013).
[19] T. Yagasaki, M. Matsumoto, and H. Tanaka, Phys. Rev. E **89**, 020301 (2014).
[20] K. Binder, Proc. Natl. Acad. Sci. U. S. A. **111**, 9374 (2014).
[21] Y. Suzuki and O. Mishima, Phys. Rev. Lett. **85**, 1322 (2000).
[22] Y. Suzuki and O. Mishima, J. Chem. Phys. **138**, 084507 (2013).
[23] Y. Suzuki and O. Mishima, J. Chem. Phys. **141**, 094505 (2014).
[24] Y. Suzuki and O. Mishima, J. Chem. Phys. **145**, 024501 (2016).
[25] Y. Suzuki, J. Chem. Phys. **147**, 064511 (2017).
[26] L. Xu, P. Kumar, S. V Buldyrev, S.-H. Chen, P. H. Poole, F. Sciortino, and H. E. Stanley, Proc. Natl. Acad. Sci. U. S. A. **102**, 16558 (2005).
[27] L. Liu, S.-H. Chen, A. Faraone, C.-W. Yen, and C.-Y. Mou, Phys. Rev. Lett. **95**, 117802 (2005).
[28] Y. Zhang, A. Faraone, W. a Kamitakahara, K.-H. Liu, C.-Y. Mou, J. B. Leao, S. Chang, and S.-H. Chen, Proc. Natl. Acad. Sci. U. S. A. **108**, 12206 (2011).
[29] A. Nagoe, Y. Kanke, M. Oguni, and S. Namba, J. Phys. Chem. B **114**, 13940 (2010).
[30] O. Mishima, J. Chem. Phys. **123**, 154506 (2005).
[31] O. Mishima, J. Chem. Phys. **126**, 244507 (2007).
[32] Y. Suzuki, Phys. Rev. B **70**, 172108 (2004).
[33] G. N. Ruiz, L. E. Bove, H. R. Corti, and T. Loerting, Phys. Chem. Chem. Phys. **16**, 18553 (2014).
[34] F. Mallamace, C. Corsaro, D. Mallamace, C. Vasi, S. Vasi, and H. E. Stanley, J. Chem. Phys. **144**, 064506 (2016).
[35] L. Le and V. Molinero, J. Phys. Chem. A **115**, 5900 (2011).
[36] D. Corradini and P. Gallo, J. Phys. Chem. B **115**, 14161 (2011).
[37] D. A. Jahn, J. Wong, J. Bachler, T. Loerting, and N. Giovambattista, Phys. Chem. Chem. Phys. **18**, 11042 (2016).
[38] J. Bachler, V. Fuentes-Landete, D. A. Jahn, J. Wong, N. Giovambattista, and T. Loerting, Phys. Chem. Chem. Phys. **18**, 11058 (2016).
[39] I. Popov, A. Greenbaum (Gutina), A. P. Sokolov, and Y. Feldman, Phys. Chem. Chem. Phys. **17**, 18063 (2015).
[40] O. Andersson and A. Inaba, J. Phys. Chem. Lett. **3**, 1951 (2012).
[41] J. W. Biddle, V. Holten, and M. A. Anisimov, J. Chem. Phys. **141**, 074504 (2014).
[42] S. Chatterjee and P. G. Debenedetti, J. Chem. Phys. **124**, 154503 (2006).
[43] S. Woutersen, B. Ensing, M. Hilbers, Z. Zhao, and C. A. Angell, Science **359**, 1127 (2018).
[44] C. U. Kim, M. W. Tate, and S. M. Gruner, Proc. Natl. Acad. Sci. U. S. A. **108**, 20897 (2011).
[45] S.-H. Chen, L. Liu, E. Fratini, P. Baglioni, A. Faraone, and E. Mamontov, Proc. Natl. Acad. Sci. U. S. A. **103**, 9012 (2006).
[46] F. Mallamace, C. Corsaro, P. Baglioni, E. Fratini, and S.-H. Chen, J. Phys.: Condens. Matter **24**, 064103 (2012).
[47] F. Mallamace, P. Baglioni, C. Corsaro, S.-H. Chen, D. Mallamace, C. Vasi, and H. E. Stanley, J. Chem. Phys. **141**, 165104 (2014).
[48] Y. Yoshimura and H. Kanno, J. Phys.: Condens. Matter **14**, 10671 (2002).
[49] A. Hauptmann, K. F. Handle, P. Baloh, H. Grothe, and T. Loerting, J. Chem. Phys. **145**, 211923 (2016).
[50] O. Mishima and Y. Suzuki, J. Chem. Phys. **115**, 4199 (2001).
[51] Y. Suzuki and O. Mishima, J. Chem. Phys. **117**, 1673 (2002).
[52] C. U. Kim, Y.-F. Chen, M. W. Tate, and S. M. Gruner, J. Appl. Crystallogr. **41**, 1 (2008).
[53] E. Mendelovici, R. L. Frost, and T. Kloprogge, J. Raman Spectrosc. **31**, 1121 (2000).
[54] O. Mishima, L. D. Calvert, and E. Whalley, Nature **310**, 393 (1984).
[55] O. Mishima, L. D. Calvert, and E. Whalley, Nature **314**, 76 (1985).
[56] R. Leberman and A. K. Soper, Nature **378**, 364 (1995).
[57] A. K. Soper and C. J. Benmore, Phys. Rev. Lett. **101**, 065502 (2008).
[58] Y. Suzuki and Y. Tominaga, J. Chem. Phys. **133**, 164508 (2010).
[59] G. G. Simeoni, T. Bryk, F. a. Gorelli, M. Krisch, G. Ruocco, M. Santoro, and T. Scopigno, Nat. Phys. **6**, 503 (2010).
[60] E. B. Moore and V. Molinero, Nature **479**, 506 (2011).
[61] G. Bullock and V. Molinero, Faraday Discuss. **167**, 371 (2013).
[62] R. S. Singh and B. Bagchi, J. Chem. Phys. **140**, 164503 (2014).
[63] K. Murata and H. Tanaka, Nat. Mater. **11**, 436 (2012).
[64] L.-S. Zhao, Z.-X. Cao, and Q. Wang, Sci. Rep. **5**, 15714 (2015).